

Transmission of perpendicular to grain forces using self-tapping screws

Philipp Dietsch, Chair of Timber Structures and Building Construction,
Technical University of Munich

Sebastian Rodemeier, Technical University of Munich

Hans Joachim Blaß, Timber Structures and Building Construction,
Karlsruhe Institute of Technology

Keywords: glued laminated timber, self-tapping screws, compression perpendicular to the grain, force transmission, reinforcement

1 Background and Objective

Structural details where timber is loaded in compression perpendicular to the grain are very common, e.g. beam supports or sill/sole plates. The combination of high loads to be transferred over localized areas and low capacities in compression perpendicular to the grain can make it difficult to meet the associated verifications. Fully threaded, self-tapping screws (STS) were identified as an efficient means to improve the stress dispersion into the timber (Bejtka & Blaß, 2006). STS have since then become a common application for the reinforcement of beams at supports.

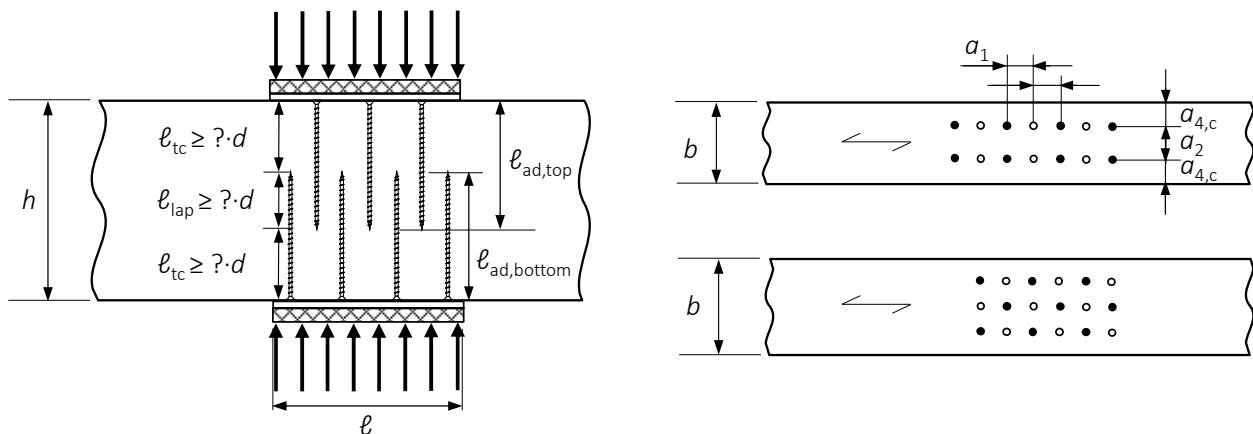


Figure 1. Self-tapping screws applied for transmission of perpendicular to grain forces.

An extended application, enabling the transfer of compression perpendicular to grain stresses through the timber member was first studied by Watson et al. (2013) for post-tensioned frame structures from LVL. Subsequently this application was introduced into one German Technical Approval (Z-9.1-519:2014). The screws are applied with an overlap, see Fig. 1, meant to transfer the compression forces from the screws on one side of the member to the screws on the opposite side. If this load transfer can be achieved, the verification of compression failure of the wood perpendicular to the grain at the screw tips can be neglected. A potential market for this application is seen in multi-story timber buildings.

During the drafting process of the new clauses on reinforcement in a revised Eurocode 5 (Dietsch & Brunauer 2017), a few questions on this application were raised, e.g. minimum overlap length, minimum distance between screw tips and opposite contact plate and arrangement of STS on opposite member edges, see Fig. 1. This paper contributes answers to these questions, based on numerical parameter studies and experiments.

2 Comparison to related structural applications

Due to the few publications dealing with the reinforcement of timber members for compression perpendicular to grain stresses up to date (see Section 1), the literature study was extended to related structural applications.

In the design of overlap joints in reinforced concrete, the type of loading (tension joint or compression joint) is taken into account as well as the effective circumference of the rebars, see Fig. 2. Required overlap lengths in compression joints in normal concrete (C20/25 ÷ C50/60) are in the range of $25 \cdot d \leq \ell_0 \leq 45 \cdot d$ with a minimum length $\ell_{0,\min} = 200 \text{ mm}$ (EN 1992-1-1:2010).

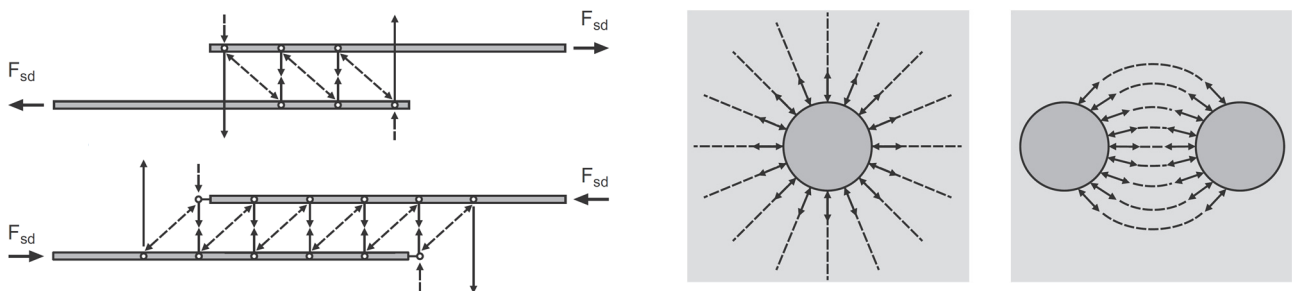


Figure 2. Structural system for the design of overlapping concrete rebars (left) and effective circumference of single rebars and overlapping rebars in concrete (Zilch & Zehetmeier, 2006).

In the design of pile foundations in geotechnical engineering, the different settlement behaviour of single piles in a group of piles (see Fig. 3) is accounted for by verifying the load-carrying capacity of the single piles as well as the load-carrying capacity of the group of piles, schematized as one single substitute pile (EN 1997-1:2013). One main design parameter in both applications is the spacing between rebars or piles.

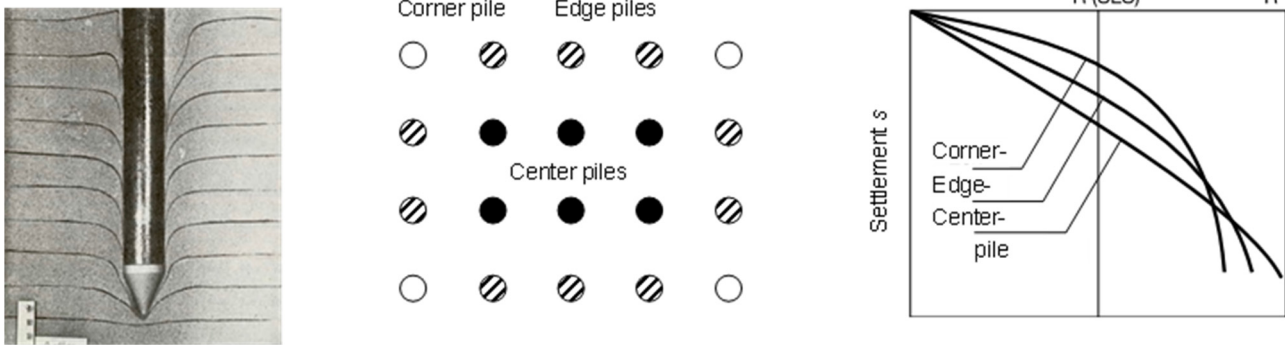


Figure 3. Failure mechanism of pile in dense sand (left; Vesic, 1977); pile categories and settlement behaviour of different pile categories in a group of piles (according to Kempfert, 2001).

3 Configuration for numerical and experimental studies

Both, intermediate supports and end supports should be investigated. The distance between screw tips and opposite contact plate, ℓ_{tc} , should be sufficient to prevent load transfer from the contact plate to the screw tips. The STS should be sufficiently long to investigate load transfer at different overlap lengths ℓ_{lap} between zero and $20 \cdot d$. The following configuration was in best agreement with the above-mentioned boundary conditions. A specimen depth of $40 \cdot d$ enabled overlap lengths ℓ_{lap} between zero ($0 \cdot d$) and half ($20 \cdot d$) of the specimen depth, while the remaining length ℓ_{tc} between the screw tips and the opposite contact plate was at least a quarter of the beam depth ($10 \cdot d \div 20 \cdot d$). Screw spacing in the area of overlap should equal the minimum required spacing ($a_1 \cdot a_2 = 25 \cdot d_1^2$ in most technical approvals) to achieve the optimum reinforcing effect. In order to reach real-size, reasonably to handle specimens, the screw diameter was chosen as $d = 8$ mm. 6 STS from the bottom and 4 STS from the top at minimum spacing were chosen, resulting in dimensions of the contact area of $\ell/b = 200/100$ mm² and specimen dimensions $h/b = 320/100$ mm².

4 Numerical parameter studies

4.1 Materials and methods

The determined configuration was realized as a parametrized 3-D FE-model (ANSYS Workbench 19.1). Glued-laminated timber GL24h (EN 14080:2013) was taken as basis for the stiffness parameters of the timber specimen. The STS were modelled as cylinders, encircled by a tube representing the transition region containing the screw thread and the wood material. The axial slip modulus of the STS, K_{ax} , is represented by the shear stiffness G of the volume. The axial slip modulus K_{ax} was derived from the modelling of associated experimental investigations (Mestek, 2011), (Danzer, Dietsch & Winter, 2016). The simulation was limited to the linear-elastic state. For verification, support areas with and without reinforcement were modelled and compared to literature (Bejtka, 2005).

4.2 Results – support with single-sided reinforcement

The results for the support area with single-sided reinforcement indicate a concentration of compression perpendicular to grain stresses between the screw tips and the opposite member edge (continuous support) with stress maxima in the plane of the screw tips, see Fig. 4.

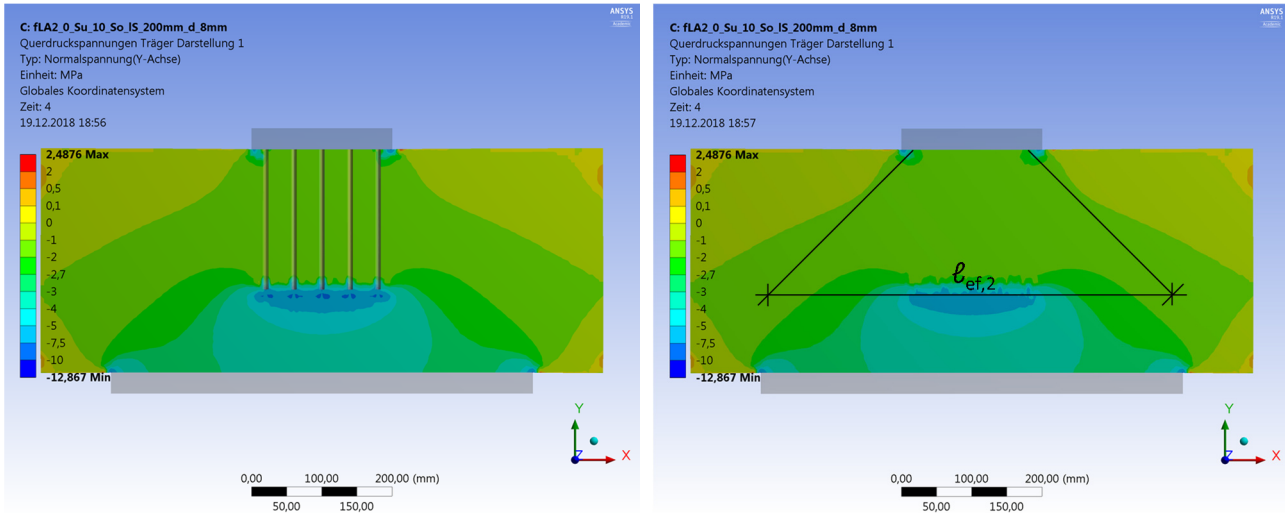


Figure 4. Distribution of compression perp. to grain stresses in reinforced support area.

An evaluation of perpendicular to grain stresses along the length $l_{ef,2}$, used for verification of compression capacity perpendicular to grain at the screw tips (e.g. ETA-12/0114:2017), indicates a considerable variation of stresses along this length with stress concentrations in the direct proximity of the screws, see Fig. 5. In the ultimate limit states, this will partly be compensated by stress redistribution due to the elastic-plastic failure mechanism of wood in compression perpendicular to the grain.

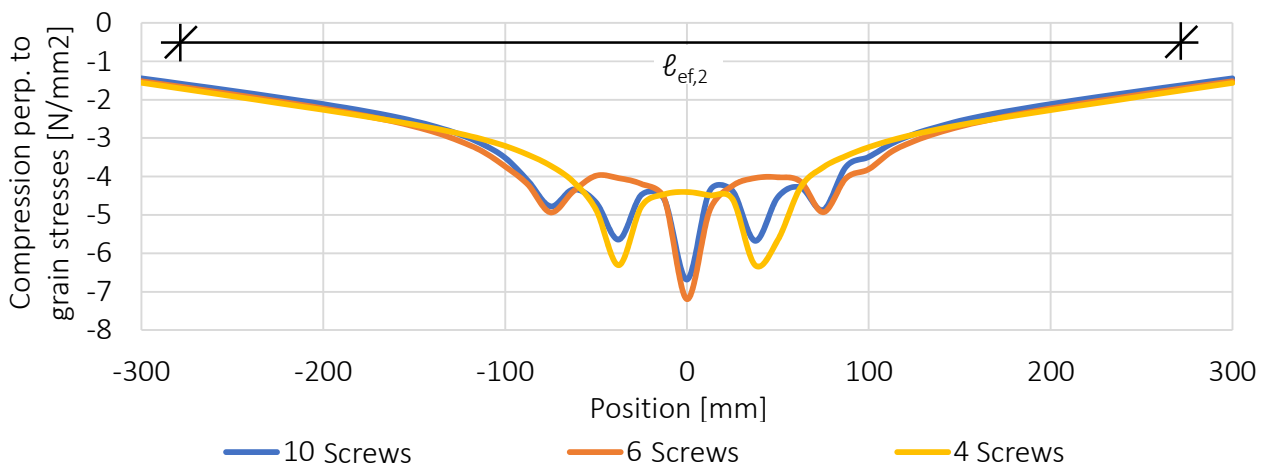


Figure 5. Distribution of compression perp. to grain stresses in horizontal plane at the screw tips.

The axial compression stresses in the screws positioned at the edges/corners of a group of screws are up to one quarter higher than the stresses in the inner screws, see Fig. 6. Reason is a group effect between the screws and the wood material inside the circumference of the group of screws, which leads to a rather homogeneous deformation of both materials. In contrast to that, the wood outside the circumference deforms less than and the group of screws, leading to higher shear between the

wood and the outer screws and hence to higher axial compression stresses in these screws. This finding correlates with the load-distribution in a group of piles in a pile foundation, see Fig. 3.

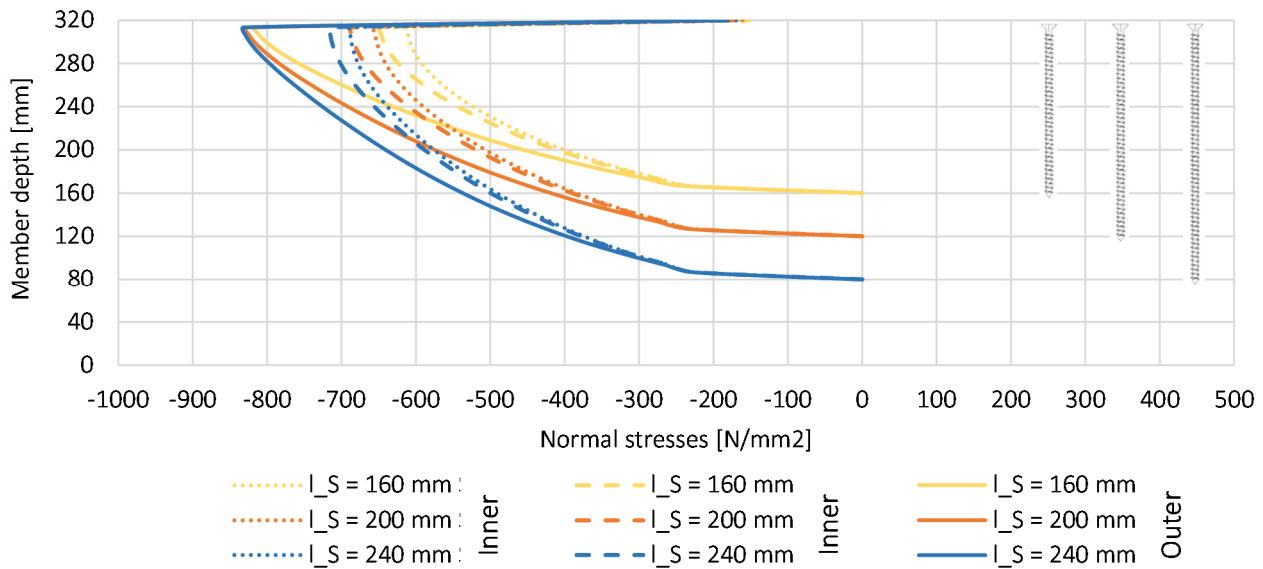


Figure 6. Distribution of axial compression stresses in outer and inner screws in a group of screws.

4.3 Results – double-sided reinforcement

When the configurations are extended to reinforcement by STS applied from opposite edges of the timber member, one additional and potentially governing parameter is given by the overlap length ℓ_{lap} . Configurations in which the screw tips end at one horizontal plane ($\ell_{lap} = 0 \cdot d$) lead to high localized deformations (and hence compression stresses) perpendicular to the grain close to the plane of the screw tips. Increasing the overlap length to $\ell_{lap} = 5 \cdot d$ already leads to a noticeable reduction, however the largest deformations still occur at the screw tips. The lowest values are observed for overlap lengths $\ell_{lap} = 10 \cdot d$, the distribution of deformations is the most homogeneous of all configurations. Overlap lengths $\ell_{lap} > 10 \cdot d$ do not lead to further reduction of deformations, the location of maximum deformations (and hence maximum compression perpendicular to grain stresses) is moved towards the contact areas on the member edges. The maximum axial compression stresses in the screws increase with increasing overlap length, however for overlap lengths $\ell_{lap} > 10 \cdot d$, this increase becomes marginal.

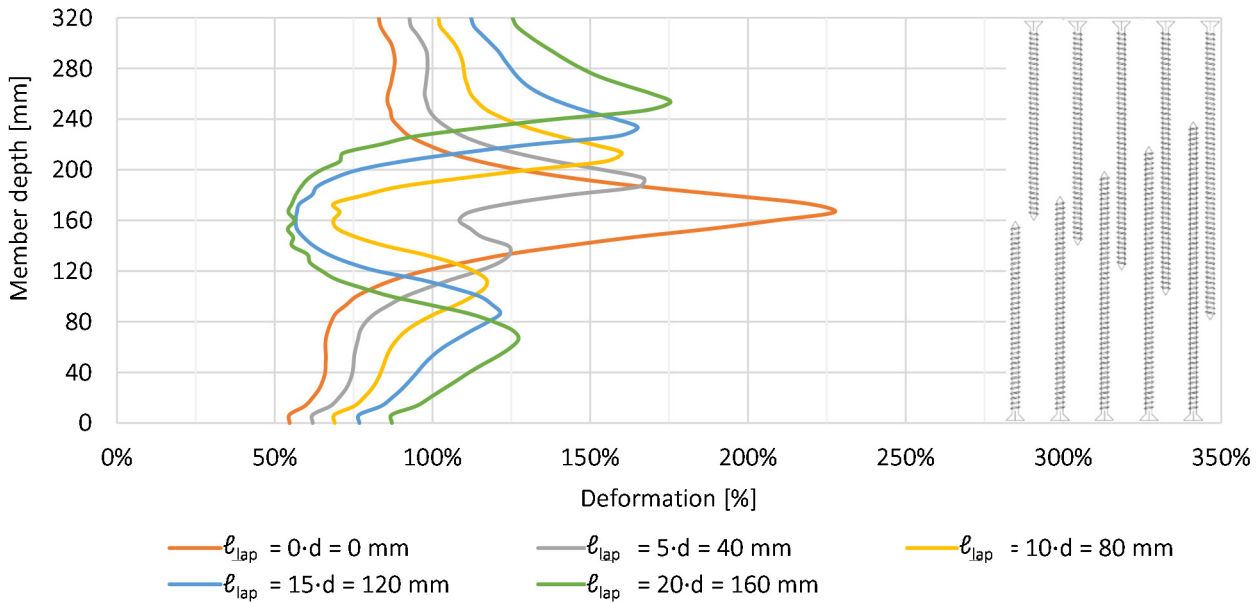


Figure 7. Deformations (percent) perpendicular to the grain over the member depth (vertical path at $b/2$) at varying overlap length ℓ_{lap} .

Fig. 8 illustrates that increasing overlap lengths also result in a reduced dispersion of compression perp. to grain stresses into the timber member, i.e. a more confined stress bulb. An increase in overlap length ℓ_{lap} leads to a reduction of the distance ℓ_{tc} between the screw tips and the opposite contact plate and to increased concentration of compression perp. to grain stresses in this area. This fact will be further discussed in the evaluation of the experimental campaign. Varying the distance ℓ_{tc} while keeping overlap lengths ℓ_{lap} constant indicates, that the increase in compression perp. to grain stresses in the area between the screw tips and the opposite contact plate becomes substantial for distances $\ell_{tc} < 15 \cdot d$. These stresses can be reduced by an alternating arrangement of the screws (alternative detail in Fig. 1) due to the more direct (i.e. increased) load transfer between two screws arranged at spacing a_2 . A variation of screw diameter only showed marginal influence on the described relationships.

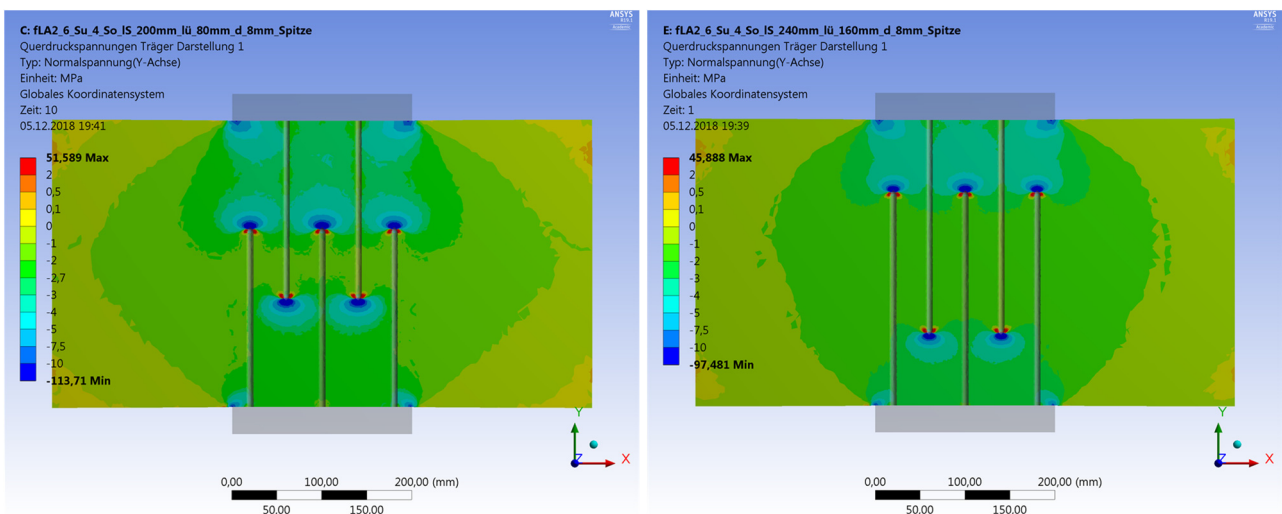


Figure 8. Compression perp. to grain stresses at overlap length $\ell_{lap} = 10 \cdot d$ (left) and $20 \cdot d$ (right).

5 Experimental campaign

5.1 Materials and methods

The experimental campaign consisted of 7 different configurations with in total 32 specimens, see Fig. 9 and Tab. 1. The first configuration, an intermediate support without reinforcement, was tested for comparative reasons. This was followed by tests on four configurations representing intermediate supports (type (a) in Fig. 9) with four STS from the top, six STS from the bottom and overlap lengths $\ell_{lap} = \{5 \cdot d, 10 \cdot d, 15 \cdot d, 20 \cdot d\}$. The sixth configuration featured an alternating arrangement of five STS each from top and bottom with $\ell_{lap} = 10 \cdot d$ (type (b) in Fig. 9), while the last configuration represented an end support (type (c) in Fig. 9) with 4 STS x 6 STS and $\ell_{lap} = 10 \cdot d$.

The self-tapping screws (ETA-12/0114:2017) featured a diameter $d = 8$ mm and lengths $\ell = \{180, 200, 220, 240$ mm}. The STS were applied using minimum required spacing, the screw heads flush with the contact surface. The glulam specimens of grade GL 24h (EN 14080:2013) featured dimensions $\ell/h/b = 600/320/100$ mm and lamella thickness $t = 40$ mm. The measured timber moisture content was $u_{mean} = 10,9$ %, the measured density was $\rho_{12\%,mean} = 444$ kg/m³, see Tab. 1.

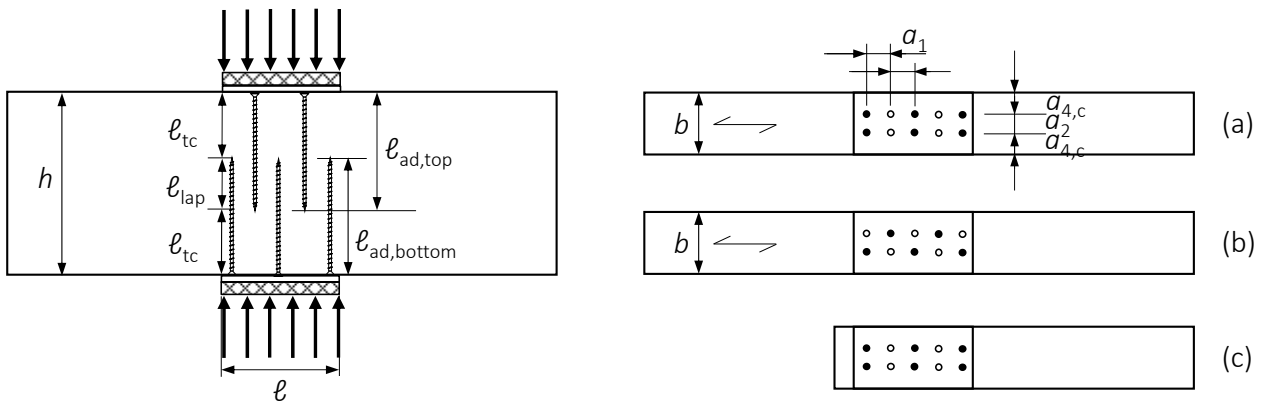


Figure 9. Overview of specimen geometry.

Table 1. Test series and information on specimens and geometry.

Series No.	1	2	3	4	5	6	7
Configuration	-	a	a	a	a	b	c
Arrangement (total-top-bottom)	no screws	10-6-4	10-6-4	10-6-4	10-6-4	10-5-5	10-6-4
Overlap length [mm]	-	$5 \cdot d = 40$	$10 \cdot d = 80$	$15 \cdot d = 120$	$20 \cdot d = 160$	$10 \cdot d = 80$	$10 \cdot d = 80$
Screw length [mm]	-	180	200	220	240	200	200
No. of specimens [-]	3	5	6	5	5	5	3
Density $\rho_{mean,12\%}$ [kg/m ³]	439	449	442	439	439	455	443
COV [%]	3,1	1,1	1,4	2,5	0,6	1,3	0,6
MC u [%]	11,0	11,0	10,9	11,0	10,7	11,0	10,9
COV [%]	1,6	0,8	1,9	2,2	2,1	2,3	2,4

The compression strength perp. to grain of the glulam was determined on five specimens $\ell/h/b = 150/200/100 \text{ mm}^3$ according to (EN 408:2012). The resulting compression strength $f_{c,90,\text{mean}} = 2,9 \text{ N/mm}^2$ and $f_{c,90,k} = 2,5 \text{ N/mm}^2$ mirrors the values given in (EN 14080: 2013) for glulam GL24h.

The tests were carried out in a universal testing machine (Zwick600E). The displacement controlled pressure load (1 mm/min) was applied via two steel plates ($\ell/b/t = 200/120/30 \text{ mm}^3$), loading the test specimens in compression perpendicular to grain. Three inductive displacement transducers (HBM WA-T) were placed at each side of the specimen to measure deformations over different parts of the specimen depth (e.g. between the two steel contact plates and within the overlap length ℓ_{lap}).

For the reinforced series, the load F_{max} was determined from the load-deformation curve. For the unreinforced series 1, F_{max} was determined according to EN 408. Reason for this choice was that the deformation of the unreinforced series 1 at F_{max} , determined according to (EN 408: 2012), was in the same range as the deformation at F_{max} of the reinforced series. For all test series, the mean modulus of elasticity perpendicular to the grain, $E_{90,\text{tot,mean}}$ was determined according to (EN 408:2012).

For a comparison with design approaches, the characteristic values of the individual test configurations, determined according to (EN 14358:2016) are compared to the load-carrying capacities determined with design approaches given in standards (EN 1995-1-1 - pushing-in capacity), Technical Assessment documents (ETA-12/0114:2017 - buckling capacity) or draft standards (PT.1 draft "reinforcement", see Dietsch & Brunauer 2017 - buckling capacity). The load-carrying capacities determined with the latter approach are very close ($\pm 1 \%$) to the load-carrying capacities determined with the comprehensive approach according to Bejtka (2005). The comprehensive approach (see also Bejtka & Blaß, 2006) was also used to determine the buckling capacity assuming clamped screw head supports. All calculations were based on a characteristic compression strength of the glulam $f_{c,90,k} = 2,5 \text{ N/mm}^2$ (EN 14080: 2013), the characteristic density determined for the test specimen $\rho_k = 428 \text{ kg/m}^3$ and a characteristic yield strength of the STS $f_{y,k} = 1000 \text{ N/mm}^2$.

5.2 Results

During the tests, the load in the reinforced test specimens initially increased linearly, see Fig. 10. Then the slope of the load-deformation curve reduced until the maximum load was reached, followed by decreasing load with increasing deformation (load reduction of 12 % - 23 %). This phase was associated with local crushing of the wood fibers below the contact plate and simultaneous failure of the STS in buckling or pushing-in at maximum load. A further increase in deformation led to a slight increase in load-carrying capacity due to the increasing activation of the wood fibers at the edges of the contact plates. Within each test series, the load-deformation curves are comparatively homogeneous in the linear elastic range but exhibit larger scatter in the plastic range. The described behavior was observed for all reinforced configurations representing intermediate supports.

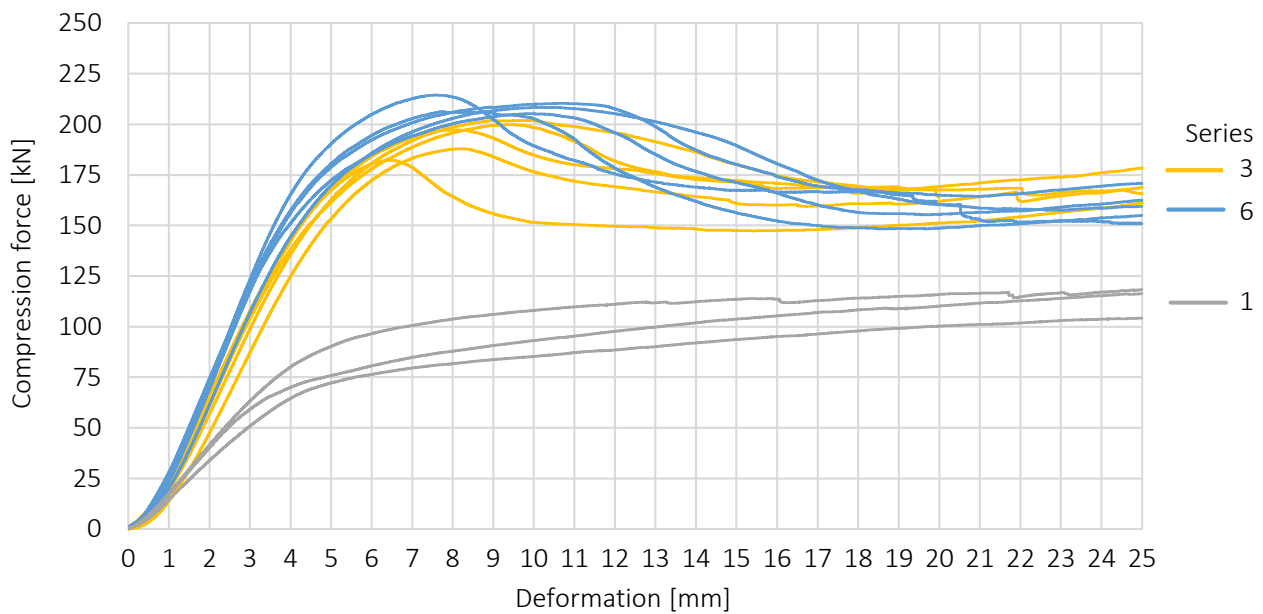
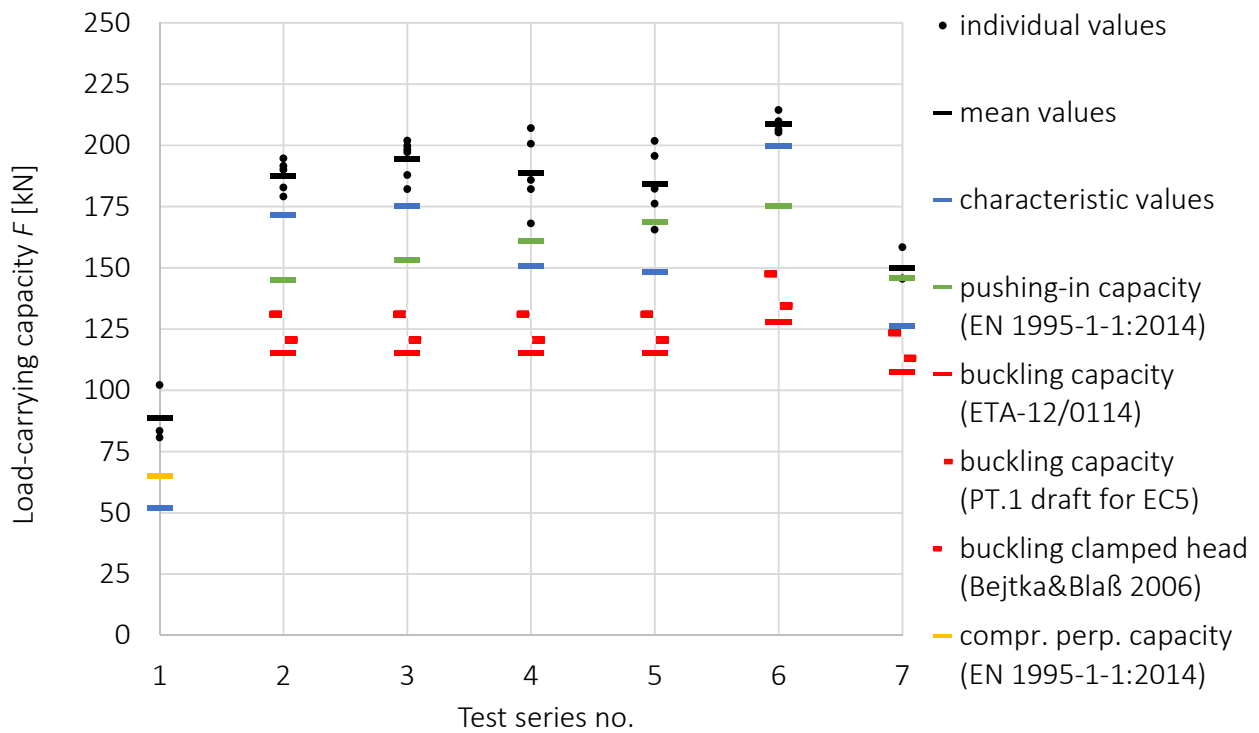


Figure 10. Force-deformation curves for series 1 (not reinforced), 3 (configuration a, $\ell_{lap}=10\cdot d$) and 6 (configuration b, $\ell_{lap}=10\cdot d$).

Four specimens each of series 2 and 3 exhibited pushing-in failure or a combination of pushing-in and buckling failure of the STS. All other specimens of series 2 – 5 exhibited essentially a buckling failure of the STS close to the screw heads (< 60 mm, i.e. $< 8\cdot d$), perpendicular to grain in direction of the nearest side face. The buckled shape of the STS indicates a clamping effect between the steel plate and the screw heads, see Fig. 12 (right). Screw buckling occurred at the beam edge featuring the smaller number of STS. Specimens of series 6 (alternative arrangement (b)) essentially exhibited a combination of pushing-in and buckling failure in vicinity of either the upper or the lower beam edge. Specimens of series 7 (end support) did not exhibit screw failure but splitting failure of the timber specimens at the end grain due to lateral extension of the wood in direction of the specimen side faces.

Fig. 10 illustrates the considerable increase in stiffness and load-carrying capacity of specimens reinforced with STS applied from both member edges compared to the unreinforced configuration. This is further illustrated in Fig. 11, showing the test data (including mean and characteristic values) compared to load-carrying capacities determined with different design models.

The mean and characteristic values of the test series show a slight increase between overlap lengths $\ell_{lap} = 5\cdot d$ and $10\cdot d$ (Series 2+3), followed by a slight decrease for $\ell_{lap} = 15\cdot d$ and $20\cdot d$ (Series 4+5) with increasing COV. The best results are determined for an alternating arrangement of the screws. The mean values of series 6 are 7 % higher than the mean values of the corresponding arrangement of series 2, in addition, the COV is considerably reduced. The mean load carrying capacity of reinforced end supports (series 7) is 23 % below the mean load-carrying capacity of the comparable intermediate support (series 2). The mean load-carrying capacities of the reinforced configurations with $\ell_{lap} = 10\cdot d$ are 119 % resp. 135 % (series 3+6) higher compared to the unreinforced configuration (series 1).



F_{mean} [kN]	88,7	187,6	194,6	188,7	184,3	208,8	149,9
COV [%]	13,2	3,4	4	8,2	8,0	1,7	4,9
F_{char} [kN]	51,9	171,8	175,5	150,7	148,3	200	126,6
$E_{90,\text{tot,mean}}$	395	805	839	929	1048	992	813
COV [%]	13,1	10,6	8,2	10,2	1,6	5,6	2,0

Figure 11. Comparison of test results with design approaches and numerical values from test series.

A comparison with the available design approaches shows that the characteristic values of test series 2, 3 and 6 are above the values determined with the design approaches. Due to the larger COV determined for series 4 and 5, the characteristic values of the test series are above the calculated buckling capacities but below the calculated pushing-in capacities of the STS.

The majority of the screws failed in buckling perpendicular to the grain in direction of the nearest side face of the specimen. This mirrors the relationships determined with the design approaches. A comparison of test series 3 – 5 shows a decreasing load-carrying capacity with decreasing distance ℓ_{tc} {15·d, 12,5·d, 10·d}. The deformation measurements showed that a reduction of the distance ℓ_{tc} leads to a concentration of deformations in this area and hence increasing strains between the screw tips and the opposite contact plate. The resulting compression perp. to grain stresses lead to lateral extension of the wood. This deformation reduces the horizontal elastic foundation c_h of the screws in this area and hence reduces the buckling load in the zone of highest axial compression stresses in the STS. Fig. 12 illustrates this behaviour. The test results in combination with the numerical results (see Fig. 7) indicate that the distance between screw tips and the opposite contact plate at the beam should be at least $\ell_{\text{tc}} = 15 \cdot d$.



Figure 12. Sketch of deformation behaviour (left), lateral extension of specimen below the contact plate (middle), buckling of STS perpendicular to the grain (right).

The tested end supports did not exhibit failure of the screws but splitting failure of the wood due to lateral extension in direction of the specimen side faces. The mean load-carrying capacities are above the buckling capacities of the STS and the capacities of the timber in compression perp. to grain at the screw tips ($\ell_{ef,2}$ with $F_{c,90,k} = 90$ kN) but below the pushing-in capacities determined with standardized approaches.

The reinforced configurations exhibit an effective modulus of elasticity $E_{90,tot,ef}$ which is at least doubled compared to series 1 without reinforcement, see Fig. 11. Series 6 featuring the alternative arrangement, exhibits the best relation between stiffness and homogeneous deformation over specimen depth. Stiffness values calculated with the model described in (Bejtka & Blaß 2006) are on average 15 % lower than the determined values $E_{90,tot,mean}$.

6 Conclusions and recommendations for practice

The results presented in this paper show that self-tapping screws applied from opposite member edges and featuring an overlap in the area of half the member depth are an efficient means to transmit concentrated perpendicular to grain forces through timber members. The tested configurations exhibit load-carrying capacities and stiffness which are at least doubled compared to the unreinforced case. To enable good performance of such details, it is recommended to adhere to the following specifications, see also Fig. 13:

Acknowledgement

The research project was kindly supported by the Studiengemeinschaft Holzleimbau e.V., DE-Wuppertal, SPAX International GmbH & Co. KG, Ennepetal and W. u. J. Derix GmbH & Co., Niederkrüchten. Gratitude is extended to Dr.-Ing Ireneusz Bejtka for his advice during these studies.

7 References

- Bejtka, I., Blaß, H.J., Self-tapping screws as reinforcements in beam supports, CIB-W18/39-7-2, Proceedings of the international council for research and innovation in building and construction, Working commission W18 – timber structures, Meeting 39, Florence, Italy, 2006.
- Bejtka, I., Verstärkung von Bauteilen aus Holz mit Vollgewindeschrauben, Dissertation, Band 2 der Karlsruher Berichte zum Ingenieurholzbau, Lehrstuhl für Ingenieurholzbau und Baukonstruktion, Universitätsverlag Karlsruhe, 2005.
- Danzer, M., Dietsch, P., Winter, S., Reinforcement of round holes in glulam beams arranged eccentrically or in groups, Proceedings of the World Conference on Timber Engineering (WCTE 2016), Vienna, 2016.
- Dietsch, P., Brunauer, A., Reinforcement of timber structures - a new section for EC5, International Conference on Connections in Timber Engineering, Graz, Austria 2017.
- EN 408:2010+A1:2012, Timber structures – Structural timber and glued laminated timber – Determination of some physical and mechanical properties, CEN, Brussels, 2012.
- EN 1992-1:2014, Eurocode 2: Design of concrete structures - Part 1-1: General rules and rules for buildings, EN 1992-1-1:2004 + AC:2010, CEN, Brussels, 2014.
- EN 1995-1-1:2014, Eurocode 5: Design of timber structures - Part 1-1: General - Common rules and rules for buildings, EN 1995-1-1:2004 + AC:2006 + A1:2008 + A2:2014, CEN, Brussels, 2014.
- EN 1997-1:2013, Eurocode 7: Geotechnical design - Part 1: General rules, EN 1997-1:2004 + AC:2009 + A1:2013, CEN, Brussels, 2013.
- EN 14080:2013, Timber structures – Glued laminated timber and glued solid timber – Requirements, CEN, Brussels, 2013.
- EN 14358:2016, Timber structures – Calculation and verification of characteristic values, CEN, Brussels, 2016.
- ETA-12/0114:2017, European Technical Assessment, SPAX self-tapping screws for use in timber constructions, ETA-Denmark, Nordhavn, 2017.

- Kempfert, H.-G., Grundbau-Taschenbuch - Teil 3: Gründungen und geotechnische Bauwerke, 6. Auflage, Ernst&Sohn, Berlin, 2001.
- Mestek, P., Punktgestützte Flächentragwerke aus Brettsper Holz (BSP) – Schubmessung unter Berücksichtigung von Schubverstärkungen, Dissertation, Technische Universität München, 2011.
- Rodemeier, S., Querdruckverstärkung von Holzbauteilen bei beidseitiger Druckkräfteinleitung, Master's thesis, Lehrstuhl für Holzbau und Baukonstruktion, Technische Universität München, 2019.
- Vesic, A.S., Design of pile foundations. National cooperative highway research program, Synthesis of highway practice 42. Transportation research board, National research council, Washington D.C., 1977.
- Watson, C.P., van Berschoten, W., Smith, T., Pampanin, S., Buchanan, A.H., Stiffness of screw reinforced LVL in compression perpendicular to the grain, CIB-W18 / 46-12-4, Proceedings of the international council for research and innovation in building and construction, Working commission W18 - timber structures, Meeting 47, Vancouver, 2013.
- Zilch, K., Zehetmeier, G., Bemessung im konstruktiven Betonbau, Springer, Berlin, 2010.
- Z-9.1-519:2014, Allgemeine bauaufsichtliche Zulassung, SPAX-S Schrauben mit Vollgewinde als Holzverbindungsmittel, Deutsches Institut für Bautechnik, Berlin, 2014.